

A 10–60-GHz Micromachined Directional Coupler

Stephen V. Robertson, *Member, IEEE*, Andrew R. Brown, *Student Member, IEEE*,
Linda P. B. Katehi, *Fellow, IEEE*, and Gabriel M. Rebeiz, *Fellow, IEEE*

Abstract—A 20-dB directional coupler has been designed and fabricated on a thin dielectric membrane using micromachining techniques. The fabrication process is compatible with monolithic microwave integrated-circuit (MMIC) techniques, and the coupler can be integrated into a planar-circuit layout. Design of the asymmetric tapered coupled-line coupler relies on simple quasi-static models and ideal transmission-line theory. The use of membrane technology results in less than 0.5-dB insertion loss in the coupler from 10 to 60 GHz. In addition, a micromachined packaging technique creates a shielded circuit, which is extremely compact and lightweight.

Index Terms—Directional coupler, integrated circuits, membrane, micromachined, millimeter wave.

I. INTRODUCTION

MEMBRANE-SUPPORTED transmission lines and circuits have proven to be excellent candidates for millimeter-wave applications where conventional substrate-supported architectures begin to suffer from parasitic effects at the dielectric/air interface [1]–[3]. The transmission-line architecture in this paper is known as shielded membrane microstrip (SMM), and it has been used to realize high-performance planar components for applications up to 110 GHz [1], [2]. The SMM line is compatible with monolithic-microwave integrated-circuit (MMIC) processing techniques, and also provides the benefit of an integrated conformal package, which enhances circuit performance while substantially reducing size and cost.

This paper presents an asymmetric tapered coupled-line coupler, which is derived from the Klopfenstein impedance taper [5]. This type of coupler can be designed for any desired coupling level and it has a theoretically infinite bandwidth due to its high-pass frequency response. In practice, of course, it is impossible to achieve infinite bandwidth, especially in coupled-line structures since differences in even- and odd-mode phase velocities contribute to reduced directivity [6]. Typically, planar couplers based on tapered coupled lines can achieve 10–12-dB directivity in the 40–50-GHz frequency range by printing the lines on opposing sides of a low-

permittivity substrate.^{1,2} This method is limited by high insertion losses and the inability to integrate the coupler into millimeter-wave integrated circuits.

The research presented here seeks to extend the useful frequency range of a coupled-line coupler by equalizing the even- and odd-mode phase velocities within the coupler. A membrane-supported circuit architecture such as the SMM line will be used to create a low-permittivity environment in which both even and odd modes will propagate at the same velocity. In addition, the asymmetric tapered coupled-line coupler will be fabricated using silicon micromachining technology to maintain compatibility with MMIC processing techniques.

II. SMM

The SMM transmission line, seen in Fig. 1, utilizes micromachining processing techniques in two ways. First, the benefits of extremely low-loss and wide-band single-mode performance are provided by suspending the signal conductors in air on a very thin dielectric membrane. The membrane comprises three dielectric layers, which are grown individually using standard silicon processing techniques. The SiO₂/Si₃N₄/SiO₂ composite structure has a thickness of approximately 1.5 μm, and remains suspended when the silicon substrate is selectively removed beneath it. Second, the SMM line is a self-packaged architecture since the ground plane of the line is created by micromachining a separate shield wafer. The ground-plane cavity can be defined conformally, such that inherent isolation between neighboring transmission lines is achieved. Additionally, the use of a separate micromachined shield wafer allows selection of the ground-plane height independently of the circuit-wafer thickness. The circuit wafer and the shield wafer are bonded together using a conductive epoxy, and the assembly is attached to a metallized support wafer to complete the electrical shielding of the circuit.

Selective silicon etching is accomplished with ethylenediamine pyrocatechol (EDP) [7]. The EDP etchant solution is anisotropic, with a high selectivity to the {111} crystal planes; hence, the angled cavity sidewalls seen in Fig. 1. The EDP solution also provides excellent selectivity to the dielectric materials used to form the membranes and the titanium and gold films used to define the circuit patterns.

Propagation characteristics for an SMM line in the frequency range of 2–118 GHz were measured with an HP 8510C network analyzer and the combination of results from three

Manuscript received March 23, 1998; revised August 7, 1998. This work was supported by NASA and by the Army Research Office.

S. V. Robertson was with the Radiation Laboratory, Electrical Engineering and Computer Science Department, The University of Michigan at Ann Arbor, Ann Arbor, MI 48109-2122 USA. He is now with Lucent Technologies, Whippany, NJ 07981-0903 USA.

A. R. Brown, L. P. B. Katehi, and G. M. Rebeiz are with the Radiation Laboratory, Electrical Engineering and Computer Science Department, The University of Michigan, Ann Arbor, MI 48109-2122 USA (e-mail: rebeiz@eecs.umich.edu).

Publisher Item Identifier S 0018-9480(98)08329-X.

¹Narda, Lockheed Martin Microwave, Hauppauge, NY 11788.

²M/A-COM, Inc., Lowell, MA 01854.

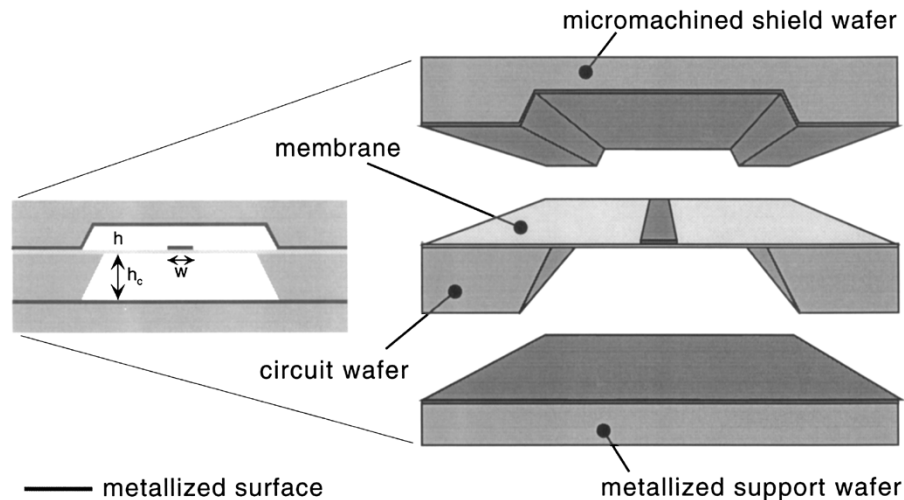


Fig. 1. Architecture of the SMM transmission line. w = strip width, h = ground plane height, and h_c = shield height.

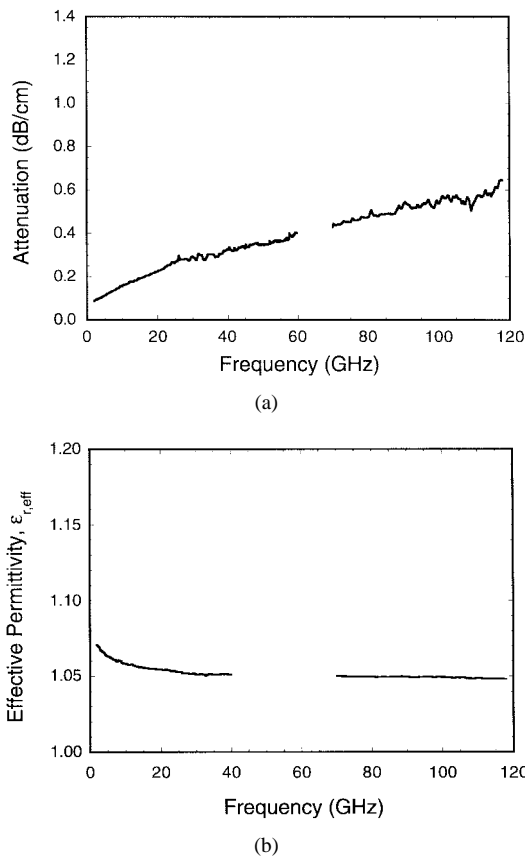


Fig. 2. Measured characteristics of an SMM line with $w = 98 \mu\text{m}$, $h = 50 \mu\text{m}$, and $h_c = 500 \mu\text{m}$. (a) Attenuation factor in decibels/centimeter and (b) effective permittivity $\epsilon_{r,\text{eff}}$. Gaps appear where data obtained from different S -parameter test sets do not overlap.

different testbands: 2–40, 40–60, and 75–110 GHz. MultiCal³ was used with on-wafer calibration standards to deembed the effects of the wafer probes, cables, etc. The line was fabricated with a ground-plane separation h of $50 \mu\text{m}$, and a cover height h_c of $500 \mu\text{m}$. A strip width w of $100 \mu\text{m}$ resulted in a nominal $90\text{-}\Omega$ characteristic impedance. Fig. 2(a) shows the

³R. B. Marks and D. F. Williams, Program MultiCal, rev. 1.00, NIST, Boulder, CO, Aug. 1995.

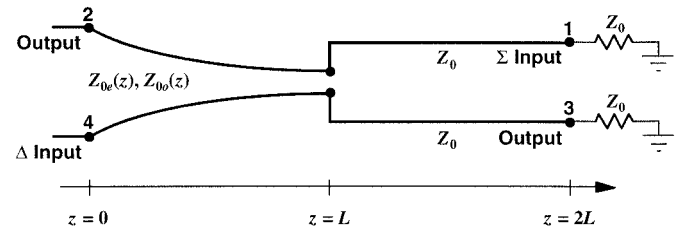


Fig. 3. Circuit schematic of the asymmetric tapered coupled line coupler. The impedance distributions $Z_{0e}(z)$ and $Z_{0o}(z)$ are calculated from the Klopfenstein taper algorithm.

measured attenuation factor, which increases as the square root of frequency due to conductor loss and is less than 0.06 dB/mm at 110 GHz . Measured effective relative permittivity data, plotted in Fig. 2(b), shows that the thin dielectric membrane causes the permittivity to increase to approximately 1.05 . The permittivity fluctuates only very slightly with frequency, indicating nearly nondispersive single-mode propagation up to 118 GHz .

III. DESIGN AND SIMULATION

Design of the SMM directional coupler is based on ideal transmission-line theory and follows the procedure presented in [8]. A schematic of the coupler circuit is illustrated in Fig. 3, and a photograph of the actual micromachined coupler (with the shield wafer removed for viewing) appears in Fig. 4. The length of the coupler L is set to 4.5 mm to provide 20-dB coupling for frequencies above 20 GHz . The method given by Grossberg [9] is used to calculate the Klopfenstein impedance values for the taper at discrete positions along the coupler. In the absence of an existing model for SMM line impedances, approximate line dimensions were synthesized using the microstrip line (MLIN) and microstrip coupled line (MCLIN) models available in HP-Eesof LineCalc.⁴ It has been previously observed that the effects of the dielectric membrane can be included in the synthesis by using a very low-permittivity substrate in the model [1]. For the SMM

⁴Hewlett-Packard Company, Santa Clara, CA 95054.

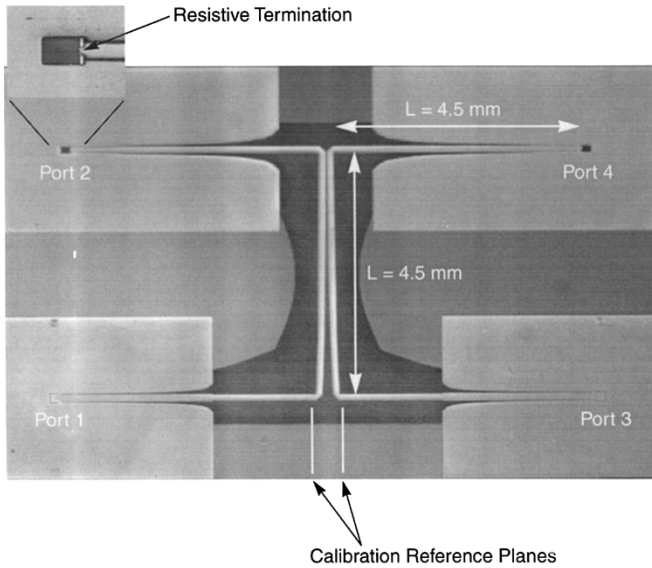


Fig. 4. Photograph of the micromachined coupler. The membrane supported region appears darker than the surrounding silicon support rim, maximum dimensions are 6 mm × 10 mm. This configuration was used to measure the coupled-port (port 3) output of the coupler; the direct (port 2) and isolated (port 4) ports are matched with on-wafer resistive terminations.

geometry used here, the synthesis model assumes a substrate with a relative permittivity of 1.05, a thickness of 50 μm , and a shield cover height of 500 μm . At each discrete position, the model is used to synthesize line dimensions from the impedances given in the Klopfenstein distribution. The layout of the coupler is generated through a piecewise-linear combination of the discrete synthesis points (see Fig. 4).

To simulate the coupler performance, a more rigorous model of the SMM coupled lines is employed. This involves the use of a two-and-one-half-dimensional (2.5-D) model of the coupled SMM lines using IE3D.⁵ The physical dimensions of the thin dielectric membrane are explicitly specified in this model so that differences in the even- and odd-mode phase velocities can be predicted. The membrane is represented as a uniform sheet with a relative dielectric constant of 4.5 and a thickness of 1.5 μm . The value of the dielectric constant of the sheet is verified by simulating a 500- μm length of the 100- μm -wide SMM line and comparing the dispersion curve obtained from the analysis with that produced from the measured data [recall Fig. 2(b)]. This predicts an $\epsilon_{r,\text{eff}}$ of 1.05 and a characteristic impedance of 90 Ω , in agreement with the original LineCalc results.

To find the mode velocity differences that exist in the coupler, each piecewise-linear section of the coupler is analyzed separately as a 500- μm length of SMM coupled lines using IE3D. The even- and odd-mode parameters (Z_{0o} , Z_{0e} , v_o , v_e) of each coupled-line section are extracted from the IE3D results and partially listed in Table I. Note that k_o and k_e are equal in regions of the coupler where the line separation is large; this shows that the presence of the membrane impacts both modes in an approximately equal manner so that they maintain equal velocities. At the opposite end of the coupler, where the line separation is very small, the impact of the

⁵Zeland Software, Fremont, CA 94538.

TABLE I
EVEN- AND ODD-MODE PARAMETERS OF THE COUPLED SMM LINES AT VARIOUS STAGES IN THE MICROMACHINED COUPLER (EXTRACTED FROM IE3D SIMULATIONS OF 500- μm -LONG COUPLED-LINE SECTIONS)

| Position (mm) | width, w (μm) | separation, s (μm) | Z_{0o} (Ω) | Z_{0e} (Ω) | k_o | k_e |
|---------------|------------------------------|-----------------------------------|-----------------------|-----------------------|-------|-------|
| 0.0 | 98 | 218 | 83.0 | 88.0 | 1.07 | 1.07 |
| 1.0 | 97 | 133 | 81.7 | 92.0 | 1.08 | 1.06 |
| 2.0 | 96 | 91 | 78.7 | 95.8 | 1.09 | 1.05 |
| 2.75 | 95 | 71 | 76.6 | 98.6 | 1.10 | 1.05 |
| 3.5 | 94 | 57 | 74.5 | 101.2 | 1.11 | 1.05 |
| 4.0 | 94 | 51 | 73.1 | 102.4 | 1.12 | 1.05 |
| 4.5 | 93 | 46 | 71.6 | 103.2 | 1.13 | 1.05 |

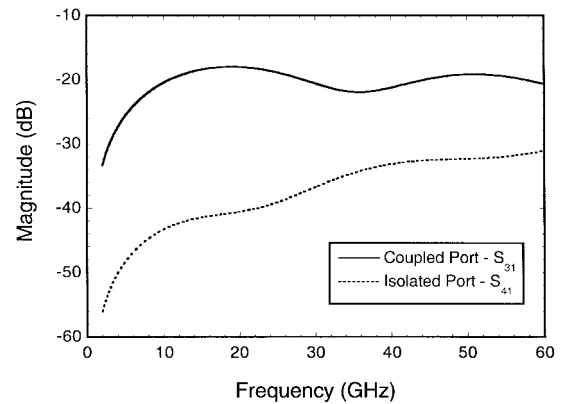


Fig. 5. Simulated response of the SMM coupler using the quasi-static model based on coupled-line parameters derived from the 2.5-D full-wave analysis.

membrane on each mode is very different. For the even mode, in which the electric fields are essentially perpendicular to the plane of the membrane, there is still very little interaction with the membrane and the propagation constant stays very close to unity. However, for the odd mode, the strong horizontal component of the electric-field distribution becomes more concentrated within the dielectric membrane, resulting in an increase in the propagation constant.

The circuit is analyzed quasi-statically with Libra by expressing the coupler as a stair-step connection of 14 lossy coupled transmission line (CLINP) elements. The CLINP elements allow specification of the mode phase velocities derived from the IE3D simulations in terms of k_e and k_o , the even- and odd-mode effective permittivities. A plot of the simulated coupling and isolation responses appears in Fig. 5, which shows the desired 20-dB coupling from 10 to 60 GHz, with a minimum directivity of 10 dB at 60 GHz.

IV. MEASUREMENTS

Deembedded on-wafer measurements of the micromachined coupler are obtained using an HP 8510C network analyzer and the MultiCal program from NIST,³ which employs the thru-reflect-line (TRL) method [10] of on-wafer calibration. On-wafer circuit contact is made via Picoprobe ground-signal-ground-type probes with 150- μm

pitch.⁶ Transition from the coplanar probe pad to the SMM geometry of the coupler is achieved through a Klopfenstein taper, which also acts to transform the 50- Ω impedance of the probes to the 90- Ω impedance of the coupler [11]. The effects of the substrate-to-membrane Klopfenstein taper are deembedded from the measurements since the TRL calibration establishes the measurement reference plane approximately 2 mm from the end of the taper (roughly 4 mm from the probe contact point).

To measure the full four-port characteristics of the coupler using only a two-port network analyzer, three identical couplers were fabricated, each designed for a different two-port measurement. On-wafer terminations were used to match the unmeasured ports of each test circuit. The on-wafer termination comprised a microshield Klopfenstein taper matched with thin-film resistors. The taper was designed to transform the 90- Ω SMM impedance to a 70- Ω microshield impedance, and two thin-film resistors were placed in parallel across the slots of the microshield line to form a 70- Ω load. The two 15 μm \times 70 μm resistors were printed via e-beam evaporation of Nichrome (Ni-Cr alloy, 40% Cr by weight) to a thickness of 700 \AA . Independent measurement of a termination (with $\approx 76\text{-}\Omega$ DC resistance) shows that the return loss exceeds 15 dB up to 60 GHz.

The measured S -parameters of the micromachined coupler (see Fig. 4) are plotted in Fig. 6. The simulated response presented in this plot is produced by adding the measured response of the on-wafer terminations to the ideal coupler response presented in Fig. 5. The measured coupling response (S_{31}) is 20.1 ± 2.5 dB from 10 to 60 GHz, and agrees very well with the simulations. The measured isolation response (S_{41}) is significantly higher than expected, resulting in a measured minimum directivity of only 5–6 dB at 52 GHz. The results of Fig. 5 indicate that a directivity of at least 10 dB should be expected from this coupler at 60 GHz. A significant portion of this discrepancy can be attributed to the loss of measurement accuracy imposed by the nonideal on-wafer terminations. Addition of the termination response to the Libra simulations results in a significant decrease in the predicted directivity, leading to the conclusion that a reduction in the return loss of the on-wafer termination would provide a more accurate measurement of the directivity. The insertion loss (S_{21}) of the coupler, plotted separately in Fig. 7, is less than 0.5 dB up to 60 GHz.

V. DISCUSSION AND CONCLUSIONS

A wide-band self-packaged micromachined directional coupler is presented. The coupler is fabricated using MMIC-compatible techniques and is completely shielded within a small lightweight micropackage. It demonstrates 20.1 ± 2.5 -dB coupling with less than 0.5-dB insertion loss from 10 to 60 GHz. The isolation response at the higher frequencies (40–60 GHz) was limited by the unequal phase velocities of the even and odd modes. This was due to the influence of the thin dielectric membrane, which caused a slight decrease in the even-mode phase velocity as compared to the odd-mode

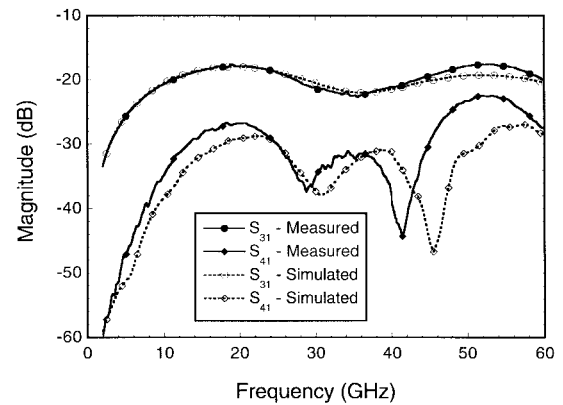


Fig. 6. Measured and simulated coupled-port and isolated-port performance of the micromachined coupler.

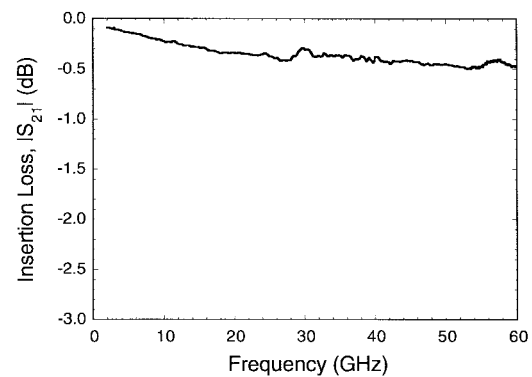


Fig. 7. Measured direct port output (S_{21}) of the micromachined coupler.

phase velocity. According to simulated results, a 5% difference between v_e and v_o can cause significant degradation in the coupler directivity, and Table I shows that this occurs for $s \leq 75 \mu\text{m}$. In future designs, it would be advantageous to choose a larger ground-plane separation in order to maximize s at the narrow end of the coupler. Note that h should not be chosen so large as to make the line separation impossibly wide at the opposite end of the coupler.

ACKNOWLEDGMENT

The authors wish to thank Dr. R. N. Simons, NASA Lewis Research Center, Cleveland, OH, and Dr. R. F. Drayton, University of Illinois at Urbana-Champaign, Chicago, for their helpful discussions.

REFERENCES

- [1] S. V. Robertson, L. P. B. Katehi, and G. M. Rebeiz, "Micromachined self-packaged W -band bandpass filters," in *IEEE MTT-S Dig.*, Orlando, FL, May 14–19, 1995, pp. 1543–1546.
- [2] C.-Y. Chi and G. M. Rebeiz, "Planar microwave and millimeter-wave lumped elements and coupled-line filters using micro-machining techniques," *IEEE Trans. Microwave Theory Tech.*, vol. 43, pp. 730–738, Apr. 1995.
- [3] T. M. Weller, L. P. B. Katehi, M. I. Herman, and P. D. Wamhof, "Membrane technology (MIST-T) applied to microstrip: A 33 GHz Wilkinson power divider," in *IEEE MTT-S Dig.*, San Diego, CA, May 23–27, 1994, pp. 911–914.
- [4] R. F. Drayton and L. P. B. Katehi, "Development of self-packaged high frequency circuits using micromachining techniques," *IEEE Trans. Microwave Theory Tech.*, vol. 43, pp. 2073–2080, Sept. 1995.

⁶GGB Industries, Inc., Naples, FL 34104.

- [5] R. W. Klopfenstein, "A transmission line taper of improved design," *Proc. IRE*, vol. 44, pp. 31–35, Jan. 1956.
- [6] R. Levy, "Directional couplers," in *Advances in Microwaves*, Leo Young, Ed. New York: Academic, 1966, pp. 115–209.
- [7] K. E. Peterson, "Silicon as a mechanical material," *Proc. IEEE*, vol. 70, pp. 420–457, May 1982.
- [8] D. M. Pozar, *Microwave Engineering*. Reading, MA: Addison-Wesley, 1990.
- [9] M. A. Grossberg, "Extremely rapid computation of the Klopfenstein impedance taper," *Proc. IEEE*, vol. 56, pp. 1629–1630, Sept. 1968.
- [10] R. B. Marks, "A multiline method of network analyzer calibration," *IEEE Trans. Microwave Theory Tech.*, vol. 39, pp. 1205–1215, July 1991.
- [11] S. V. Robertson, L. P. B. Katehi, and G. M. Rebeiz, "Micromachined W-band filters," *IEEE Trans. Microwave Theory Tech.*, vol. 44, pp. 598–606, Apr. 1996.



Stephen V. Robertson (M'92) received the B.S.E.E. degree from the University of Texas at Austin, in 1991, and the M.S.E. and Ph.D. degrees from the University of Michigan at Ann Arbor, in 1993 and 1997, respectively.

At the University of Michigan at Ann Arbor, he was a member of the Radiation Laboratory, where his research efforts focused on the development of silicon micromachining technology for microwave and millimeter-wave circuits. In 1998, he joined the Wireless Technology Laboratory, Lucent Technologies, Whippany, NJ.

Andrew R. Brown (S'96) received the B.S.E.E. and M.S.E.E. degrees from the University of Michigan at Ann Arbor, in 1995 and 1996, respectively, and is currently working toward the Ph.D. degree in electrical engineering.

His current research involves applying micromachining techniques to achieve very low-loss transmission lines and high- Q resonant structures for millimeter-wave communication systems.

Linda P. B. Katehi (S'81–M'84–SM'89–F'95), for photograph and biography, see this issue, p. 1844.

Gabriel M. Rebeiz (S'86–M'88–SM'93–F'97), for biography, see this issue, p. 1831.